

Supplementary Information

Supplementary Methods

The classic ‘‘Ohmic’’ method to estimate synaptic conductances from intracellular data is based on temporal averaging of the passive membrane equation (Eq. 2). Under the assumption that the average membrane potential \bar{V} remains stationary, Eq. 2 yields

$$\bar{V} = \frac{E_L + (\bar{g}_e/G_L)E_e + (\bar{g}_i/G_L)E_i}{1 + \bar{g}_e/G_L + \bar{g}_i/G_L}, \quad (7)$$

where \bar{g}_e and \bar{g}_i denote the average excitatory and inhibitory conductance, respectively. Denoting the ratio between the total membrane input resistance in states without network activity and in active states with $r_{in} = R_{in}(\text{quiescent})/R_{in}(\text{active})$, one obtains

$$\frac{\bar{g}_{\{e,i\}}}{G_L} = \frac{r_{in}\bar{V} - E_L + E_{\{i,e\}}(1 - r_{in})}{E_{\{e,i\}} - E_{\{i,e\}}}. \quad (8)$$

This relation allows one to estimate the average relative contribution of inhibitory excitatory synaptic inputs in activated states. The value of r_{in} was 3 for the wake state, it was $r_{in} = 4$ for SWS up-states and $r_{in} = 5$ for REM sleep.

Conductance estimates in morphologically-reconstructed neurons

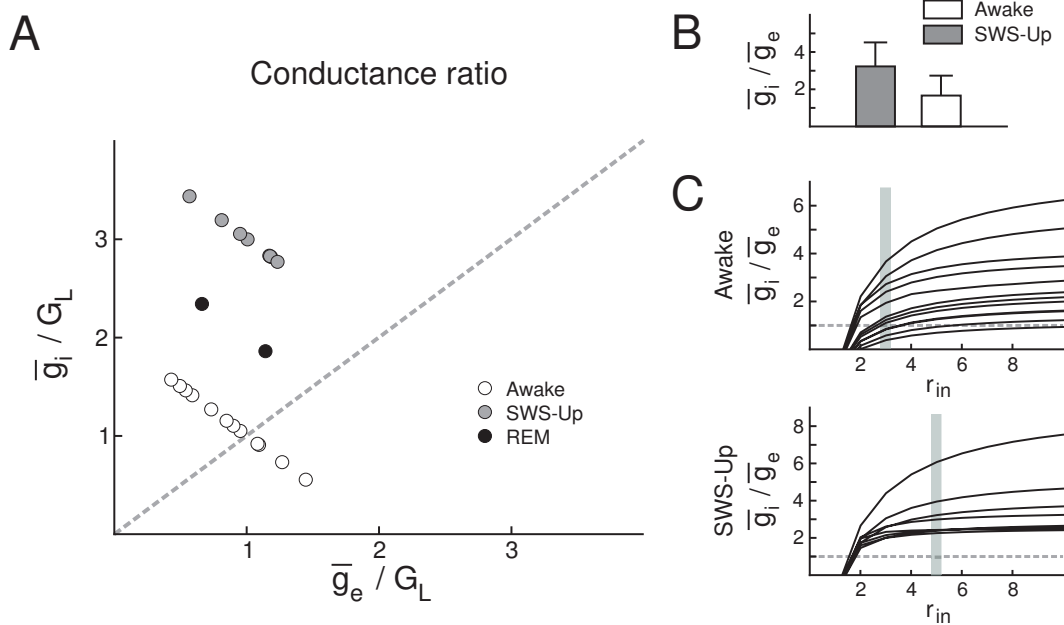
To compare the conductance analysis using the VmD method with other methods, we have performed additional simulations using models of reconstructed pyramidal neurons. In a previous study (Rudolph et al., 2004), we showed using models of pyramidal neurons that the VmD method provides conductance estimates which are identical to those obtained using a ‘‘perfect’’ (zero series resistance) voltage-clamp in the soma. We extend here these simulations by comparing VmD and voltage-clamp estimates for different parameter variations (see Supplementary Table 1). A Layer VI pyramidal cell from cat was simulated with AMPA and GABA_A synapses distributed in soma and dendrites and which released randomly such as to reproduce *in vivo*-like activity (model from Destexhe and Paré, 1999). Different situations were considered: (a) the presence of a 10 nS somatic shunt to represent sharp-electrode impalement (same parameters as in Destexhe and Paré, 1999); (b) Cesium recordings by reducing 95% of the leak conductance in soma and dendrites; (c) Different values of the series resistance of the electrode (R_s). The presence of a somatic shunt had little effect on conductance estimates, while cesium leads to larger conductances, but the largest effect was that of series resistance: not only the amplitude of the measured conductances, but also the conductance variance, and the ratio between excitatory and inhibitory conductances.

Supplementary table

	g_{e0} (nS)	σ_e (nS)	g_{i0} (nS)	σ_i (nS)	g_{i0}/g_{e0}
Control, $R_s=0$	13.41	2.68	40.66	2.79	3.03
10 nS shunt, $R_s=0$	13.44	2.68	40.66	2.78	3.03
10 nS shunt, $R_s=3 \text{ M}\Omega$	11.3	2.05	30.0	2.02	2.65
10 nS shunt, $R_s=10 \text{ M}\Omega$	8.31	1.32	15.6	1.24	1.87
10 nS shunt, Cesium, $R_s=0$	13.57	2.70	43.9	2.83	3.23
10 nS shunt, Cesium, $R_s=3 \text{ M}\Omega$	11.36	2.07	33.97	2.07	2.99
10 nS shunt, Cesium, $R_s=10 \text{ M}\Omega$	8.32	1.34	20.3	1.28	2.44
10 nS shunt, Cesium, $R_s=15 \text{ M}\Omega$	7.04	1.07	14.6	1.01	2.07
10 nS shunt, Cesium, $R_s=25 \text{ M}\Omega$	5.46	0.76	7.46	0.71	1.36

Supplementary Table 1:

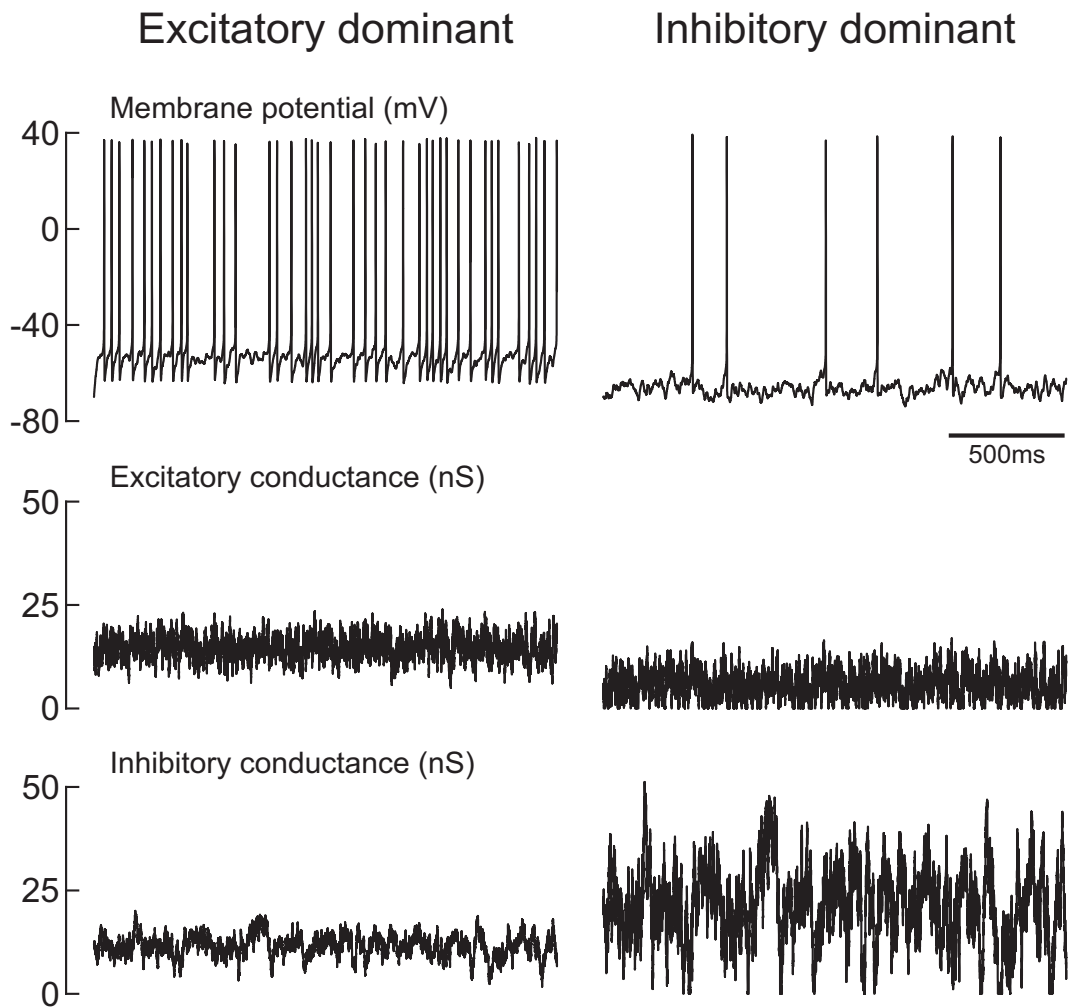
Conductance estimates in voltage-clamp using a morphologically-reconstructed cortical pyramidal neuron. A model of background activity in a spatially distributed neuron (Layer VI pyramidal cell), with AMPA/GABA_A currents in soma and dendrites, was used (same model parameters as given in Destexhe and Paré, 1999). The “Control” conditions correspond to a perfect voltage-clamp (series resistance $R_s=0$), which was used to estimate the excitatory and inhibitory conductances visible from the somatic electrode. A 10 nS shunt was added in the soma, and the series resistance was varied. To simulate recordings in the presence of Cesium, the leak resistance was reduced by 95%, but the shunt was unaffected. The last column indicates the ratio between inhibitory and excitatory conductances. Both the amplitude of the measured conductance, and the ratio of excitation/inhibition, were highly dependent on series resistance.



Supplementary Figure 2:

Estimation of relative conductances from intracellular recordings using the Ohmic method.

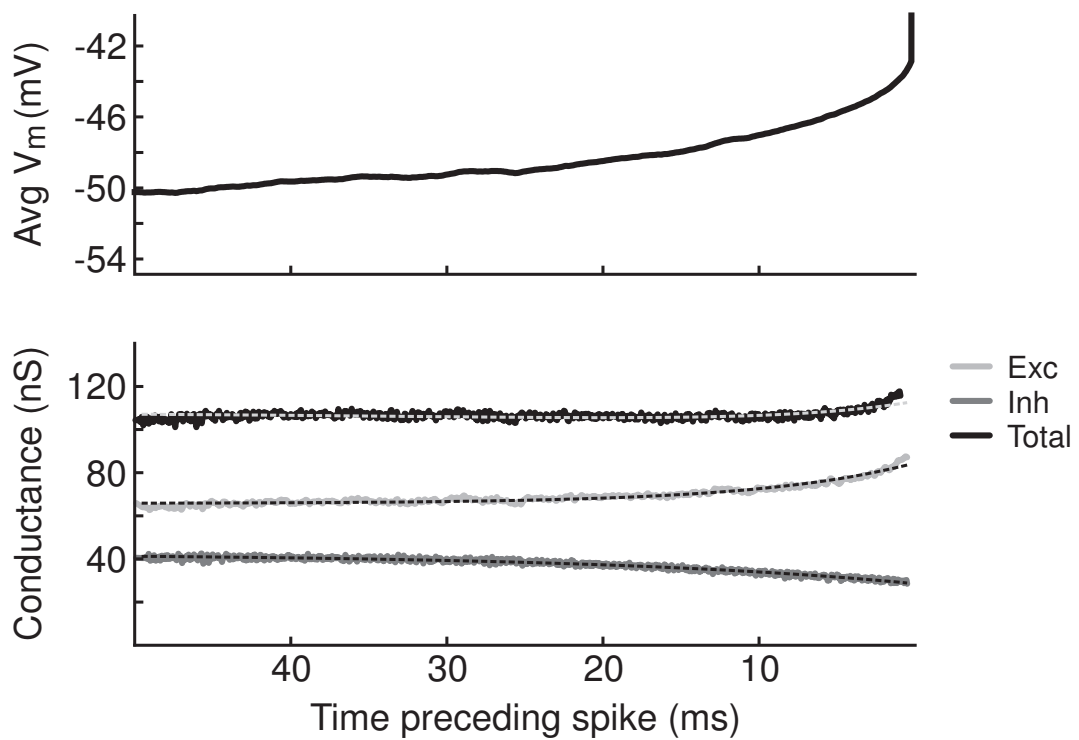
A. Contribution of average excitatory (\bar{g}_e) and inhibitory (\bar{g}_i) conductances relative to the leak conductance G_L during wakefulness (Awake), slow-wave sleep up-states (SWS-Up) and REM sleep periods. Estimates were obtained by incorporating measurements of the average membrane potential (spikes excluded) into the passive membrane equation (Ohmic method, see Supplementary Methods). Estimated relative conductance values show a high variability among the investigated cells, but a general dominance of inhibition. **B.** Average ratio between inhibitory and excitatory mean conductances observed during wakefulness (Awake) and slow-wave sleep up-states (SWS-Up). Dominant inhibition was observed in both states, and more pronounced during SWS. **C.** Variations of the ratio between average inhibitory and excitatory conductance values as a function of different choices for the leak conductance. $r_{in} = R_{in}(\text{quiescent})/R_{in}(\text{active})$; the gray area indicates the values used for conductance estimation used in **A** and **B**.



Supplementary Figure 3:

Computational models of two different conductance dynamics in the wake state.

Two examples similar to Fig. 7A are shown for conductance measurements in two other cells. Left panel: neuron where the excitatory conductance was larger than the inhibitory conductance (“Excitatory dominant”). Right panel: neuron for which the inhibition was more pronounced (“Inhibitory dominant”; this type of cell represented the majority of cells in the waking state). Same parameters as in Fig. 7A and Methods, except $g_{e0} = 14.6$ nS, $g_{i0} = 12.1$ nS, $\sigma_e = 2.7$ nS, $\sigma_i = 2.8$ nS (left panel); $g_{e0} = 5.7$ nS, $g_{i0} = 22.8$ nS, $\sigma_e = 3.3$ nS, $\sigma_i = 10.0$ nS (right panel).



Supplementary Figure 4:

Example of cell showing an increase of total membrane conductance preceding spikes during the wake state. For this particular neuron recorded during the wake state, the STA showed an increase of total membrane conductance prior to the spike. Same description of panels and curves as in Fig. 9A, Awake.